Real Time High Spatial-Temporal Resolution Flow Imaging with Spiral MRI using Auto-Calibrated SENSE

Reza Nezafat*†, Peter Kellman†, John A. Derbyshire† and Elliot R. McVeigh†*
*Department of Biomedical Engineering, Johns Hopkins School of Medicine, Baltimore, MD
†Laboratory of Cardiac Energetics, National Heart, Lung and Blood Institute, National Institute of Health, DHHS, Bethesda, MD

Abstract— **A novel spiral phase contrast technique was developed for high temporal and spatial resolution imaging of blood flow without cardiac gating. Spiral sampling of *k*-space has excellent flow properties and acquisition speed. Parallel imaging using the coil sensitivity maps can be used to reduce the imaging duration at the cost of SNR. An auto-calibrated spiral sensitivity encoding method is introduced and used for reconstruction of phase contrast images. Phase estimation for a simulated phantom using data from various acceleration rates was compared to the true phase map. To study the accuracy of the flow estimate with parallel image reconstruction, a high resolution cardiac gated experiment was performed and a subset of under-sampled data were reconstructed. The real-time experiments were performed to measure blood velocity in the ascending aorta and through the aortic valve with high spatial and temporal resolution. Temporal resolution of the flow images was improved by a factor of at least three with no cardiac gating signal with preserved spatial resolution. The results demonstrate the potential of using the technique for real-time flow imaging with improved spatial and temporal resolution.**

Index Terms— **Phase Contrast, Real-Time MRI, SENSE, Spiral**

I. Introduction

Ultrasound of the vascular system is an established technique that can be used to image blood flow. A color map of blood flow can be visualized using the frequency shift of the emitted high-frequency sound. Magnetic resonance imaging of the rapid variations of the blood flow in the vascular system has been demonstrated [1], [2], [3]. Gatehouse *et. al.* [2] developed a rapid spiral sampling combined with phase velocity mapping for real-time flow velocity imaging. Nayak *et. al.* [1] developed an interactive system in which blood flow in different directions can be imaged, fast spiral trajectories were used to sample *k*-space and a color map was used to visualize the blood flow. Thompson *et. al.* [3] proposed a real-time volumetric flow measurement technique with complex difference processing providing an integral of volumetric blood flow in a single projection. In all proposed techniques, the need for faster acquisition of the minimum required *k*-space data for reconstruction of non-aliased full FOV is demonstrated.

Parallel imaging, exploiting the coil sensitivity maps, can be used to reduce the image acquisition time while keeping the spatial resolution unchanged at the cost of SNR [4], [5]. Conjugate gradient SENSE reconstruction for arbitrary sampling trajectories has been proposed to suppress the artifacts arising from under-sampled data [6]. The accuracy and reproducibility of blood flow velocity measurements using SENSE reconstruction with Cartesian sampling at different reduction factors was studied recently and predicts an accurate estimate of the flow measurement by considering the geometry factor [7].

In the present work, a conjugate gradient SENSE reconstruction technique is used to reduce the number of spiral interleaves required for an un-aliased full FOV image for acquiring real-time blood flow measurements. An auto-calibrated acquisition scheme is proposed to construct the coil sensitivity map adaptively from the cardiac data.

II. Theory

In this section the image reconstruction technique is presented as first described by Pruessmann *et. al.* [6] and Wajer *et. al.* [8], and the a method for adaptive acquisition of the complex coil sensitivity map is discussed. Image reconstruction from multi-coil data acquired with spiral sampling is an inverse problem that can be solved approximately using an iterative method such as conjugate gradient optimization.

The RF signal $f_c(\vec{k})$ received by each receiver coil channel (*c*) in an MR experiment can be expressed as

$$\begin{aligned} f_c(\vec{k}) &= \int_{\vec{r}} \rho(\vec{r}) s_c(\vec{r}) e^{2\pi i \vec{k}\cdot\vec{r}} d\vec{r} + n_c(\vec{k}) \\ &= \int_{\vec{r}} \rho(\vec{r}) E_c(\vec{r},\vec{k}) d\vec{r} + n_c(\vec{k}) \end{aligned} \tag{1}$$

in which $s_c(\vec{r})$ is the spatial sensitivity profile of each coil that depends on the geometry of the coil and load configuration; $\vec{r}$ is the position vector in the image space and $\vec{k}$ is the *k*-space sampling trajectory which is defined as $\vec{k}(t) = k_x(t) + ik_y(t) = \lambda\theta(t)e^{i\phi(t)}$ for spiral sampling (λ is a constant which depends on imaging parameters, and $\theta(t)$ and $\phi(t)$ are smooth functions that characterize the sampling trajectories). $E_c(\vec{r},\vec{k})$ is defined as the encoding matrix. $n_i(\vec{k})$ is the receiver coil noise matrix. Finally $\rho(\vec{r})$ is the proton density of the object at the location $\vec{r}$. Equation (1) can be formulated in matrix form as:

$$F = E\rho + n \tag{2}$$

and the reconstruction problem can be expressed as finding the optimized solution for the underdetermined matrix equation

$$(E^H \Psi^{-1} E)\rho = E^H \Psi^{-1} F \tag{3}$$

In (3) the subscript H indicates the complex conjugate transpose, and Ψ denotes the sample noise matrix which depends on

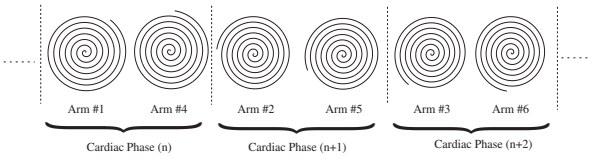

Fig. 1. Spiral interleave acquisition scheme in different cardiac phases: The fully sampled *k*-space is covered with 6-spiral interleaves and an acceleration rate of 3 is shown as an example.

the correlation of the noise between channels. If the receiver channels were decorrelated to create a set of uncorrelated virtual coils using the Cholesky decomposition of the noise correlation matrix Ψ, (3) can be simplified by replacing Ψ matrix with the Identity matrix [9]. Equation (3) can be solved for ρ using an iterative algorithm such as conjugate gradient method [9].

The right hand side of (3) can be rewritten as :

$$[E^H F](\vec{r}) = \sum_c \left\{ s_c^*(\vec{r}) \left\{ \int_{\vec{k}} \left\{ e^{-2\pi i \vec{k}\cdot\vec{r}} f_c(\vec{k}) d\vec{k} \right\} \right\} \right\} \quad (4)$$

The integral term in (4) can be calculated using the standard gridding technique [10].

To calculate the matrix-vector multiplication of $(E^H E)\rho$ during each CG iteration an efficient and fast method is implemented as suggested by Wajer et. al. [8]. The left hand side of (3) can be calculated by evaluating the component of $(E^H E)$ as follows:

$$\begin{aligned} [E^H E]_{(\vec{r},\vec{r'})} &= \sum_c \left\{ s_c^*(\vec{r}) \int_{\vec{k}} e^{-2\pi i \vec{k}\cdot(\vec{r}-\vec{r'})} s_c(\vec{r'}) d\vec{k} \right\} \\ &= \sum_c \left\{ s_c^*(\vec{r}) Q(\vec{r}-\vec{r'}) s_c(\vec{r'}) \rho(\vec{r'}) \right\} \end{aligned} \quad (5)$$

with

$$Q(\vec{r}) = \int_{\vec{k}} e^{-i\vec{k}\cdot\vec{r}} d\vec{k} \quad (6)$$

The Q function is the Fourier transform of the undersampling point spread function (PSF) that can be evaluated prior to the iteration with the gridding. Therefore the left-hand side of (3) can be evaluated using the convolution theorem as follows:

$$[E^H E \hat{\rho}_i]_r = \sum_c \left\{ s_c^*(r) [\mathcal{F}^{-1} \left\{ \mathcal{F}(Q) \ \mathcal{F}(s_c \ \hat{\rho}_i) \right\}]_r \right\} \quad (7)$$

in which $\hat{\rho}_i$ is the approximate solution for the CG after i^{th} iteration and $\mathcal{F}, \mathcal{F}^{-1}$ represent the Fourier and inverse Fourier transforms respectively.

An auto-calibrated acquisition scheme was proposed for calculation of the relative coil sensitivity maps (B_1 map) that will eliminate the acquisition of extra body and multi-coil scans. The adaptive B_1 maps can track changes that may arise from respiratory motion during the cardiac cycle. The spiral arms were interleaved in consecutive phases of the cardiac cycle and the pattern repeated after R cardiac phases (the acceleration rate) as previously demonstrated for Cartesian imaging [11], [12]. An example of the acquisition

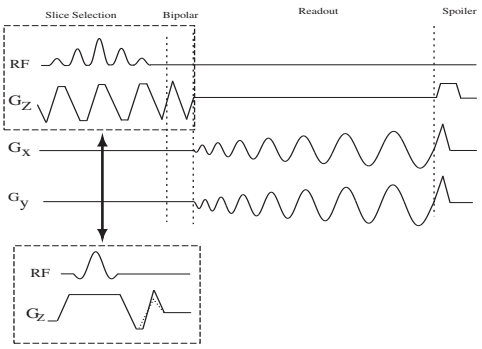

Fig. 2. Spiral phase contrast sequence with and without selective spectral-spatial RF pulse.

order for R=3 and 6 interleaves is shown in Fig. 1. A full FOV unaliased image was reconstructed by integration of the raw data over multiple cardiac phases. The temporally-filtered alias-free full FOV images were normalized by the root sum of squared magnitudes of the multiple coil images. In order to optimize SNR in the combined image and suppress the motion artifacts a spatial matched filter is used in the reconstruction of the coil sensitivity maps [13]. Local correlation statistics for each voxel were derived by cross-products over a local region in the complex image. The B_1 maps were reconstructed by calculating the eigenvector that corresponds to the maximum eigenvalue of the local correlation matrix for each voxel.

III. Method

The spiral phase contrast pulse sequence was developed by adding a pair of bipolar gradients with the desired first moment difference. The two-sided strategy for encoding a desired first moment in the PC sequence constrains bipolar flow encoding gradients to have a symmetrically placed first moment around zero gradient. Relaxing this constraint yields a shorter echo time. In other words, the first moment difference between two flow encoding steps is used as the gradient design constraint without regard to individual first moment values [14]. This gradient design scheme is used for measuring through plane flow in all experiments. The refocussing lobe in the slice select gradient was also combined with the flow encoding bipolar gradient to reduce the length of echo delay.

Image reconstruction was carried out using an iterative conjugate gradient SENSE reconstruction as described in the previous section. Individual under-sampled coil data were reconstructed using a gridding technique on a denser grid (2X over-sampling) to reduce aliasing and allowing less apodization. The gridding procedure involved a convolution with a 5×5 Kaiser-Bessel kernel followed by deapodization in the image domain [10]. The deapodization function was calculated analytically. The Fourier transform of the sampling point spread function (FQ) was constructed by gridding a unity matrix on the under-sampled trajectory with 2X over-sampling. The size of the FQ was kept twice the size of the image matrix and a zeropadded FFT of the image matrix was used for multiplication with FQ and the inverse FFT was cropped

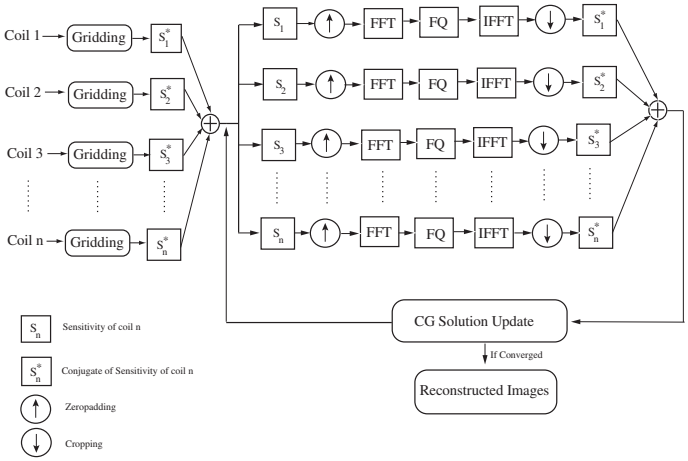

Fig. 3. Image reconstruction with conjugate gradient SENSE reconstruction

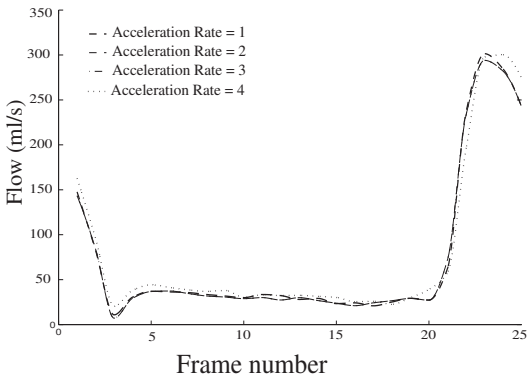

Fig. 4. Comparison of the 4 undersampling rate reconstructed with the conjugate gradient SENSE

afterward. The conjugate gradient direction were calculated using complex sum of B_1 map weighted cropped images. Fig. 3 shows a simplified diagram of the image reconstruction steps. All images were reconstructed off-line using Matlab (The Mathworks, Natick, MA). All MR experiments were performed on a GE Signa Excite 1.5T MR imaging system (GE, Waukesha, WI) with Twin gradient (maximum gradient of 4.0 G/cm, maximum slew rate of 150 G/cm/ms) using an 8-channel cardiac phased array coil (Nova Medical, Wilmington, MA) for signal detection. Normal volunteers were imaged with informed consent as approved by the NHLBI IRB. An interleaved spiral imaging sequence, that starts as a constant slew-rate and switches to a constant amplitude reaching the peak gradient amplitude [15], was modified by addition of a bipolar gradient to construct a spiral PC sequence as shown in Fig. 2. If a magnitude image in addition to the flow image is required, a water-selective spectral-spatial pulse is used for suppression of fat signals and reduction of off-resonance blurring [16].

A. Simulation Study

For validation of the phase estimation for the simulated phantom data, we compared the measured phase from the complex image of a stationary circular phantom reconstructed using conjugate gradient SENSE with different under-sampling rate to a fully sampled *k*-space image. Uniformly spaced artificial phase, ranging between $(-\pi, \pi)$, was added to a stationary phantom image with zero-phase. This image was weighted with a known sensitivity map of 8 coils to simulate the multi-coil acquisition. The complex sensitivities were calculated using Biot-Savart's law over a circular phantom. The images were transformed into *k*-space by inverse Fourier transform and resampled onto a spiral trajectory using an inverse gridding. The spiral *k*-space consisted of 6 interleaves and 1024 points per interleave and image size of 128×128. A subset of the spiral interleaves corresponding to various acceleration rates were reconstructed using the conjugate gradient SENSE reconstruction. The mean and standard deviation of the estimated phase in different ROIs in the reconstructed image were measured and compared to the induced phase.

B. In-vivo Gated Experiment

In vivo blood flow imaging studies were performed for measuring through plane blood flow in the ascending aorta. Peripheral gated cine flow acquisitions were used for measuring the blood flow. A high spatial resolution phase contrast breath-hold cine image was measured in the ascending aorta with spiral sampling with the following parameters: $TR = 25$ ms, $V_{enc} = 150$ cm/s, $\theta = 30^o$, $FOV = 30$ cm, $BW = \pm 125$ kHz, 1024 readout points and 32 spiral interleaves with an image matrix of 256×256. A single interleaf per segment was used to achieve a temporal resolution of 25 ms. Different subset of acquired data corresponding to different under-sampling rate were chosen for image reconstruction.

C. Real Time Flow in Ascending Aorta and Aortic Valve

Real-time blood flow measurement were performed for acquisition of blood flow in the ascending aorta. The acquisition parameters were as follows: $TR = 15.2$ ms, $TE = 2.3$ ms, $V_{enc} = 150$ cm/s , $\theta = 30^o$, $FOV = 34$ cm, $BW = \pm 125$ kHz, two interleaves were acquired with under-sampling rate 4 with 2048 readout-points in each interleave. A temporal resolution of 60.8 ms was achieved with these imaging parameters. For validation of the real-time measured flow, a gated experiment with the same imaging parameters was performed and the results were compared.

Through-plane blood flow through the aortic valve was imaged with no cardiac gating achieving a temporal resolution of 91.2ms with spatial resolution of 1.8mm. An acceleration rate of 3 was used with the following parameters: $TR = 15.2$ ms, $V_{enc} = 150$ cm/s, $\theta = 30^o$, $FOV = 26$ cm, $BW = \pm 125$ kHz with an image matrix of 256×256.

IV. Results

A. Simulation Study

Phase estimation of the stationary phantom was validated by comparing the reconstructed phase for 58 linearly-spaced phase increments. Fifteen ROIs in different spatial locations

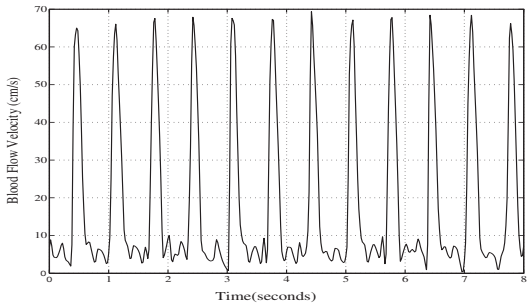

Fig. 5. Real time blood flow through ascending aorta measured with real-time spiral SENSE

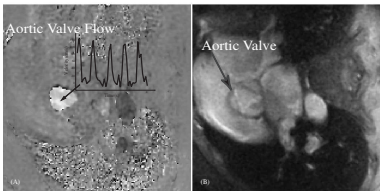

Fig. 6. Real time through plane blood flow in the aortic valve: the blood flow velocity for a sample pixel through the valve is shown in the flow image.

in the phantom were selected for calculating the mean and standard deviation of the reconstructed phase. A linear correlation analysis were performed that yielded an $r > 0.9877$ and a slope of 0.9781 for rate 2 under-sampling. The correlation analysis results in an $r > 0.9879$ and a slope of 0.9765 for rate 3 under-sampling. The spacing between different interleaves was chosen to cover the *k*-space as uniformly as possible. It was not possible to study higher under-sampling rate with the number of interleaves chosen.

B. In-vivo Gated Experiment

Cardiac gated phase contrast images were reconstructed from the the subset of the interleaves corresponding to different under-sampling rate $\{1, 2, 2.9, 4\}$. The acceleration rate 1 corresponds to B_1-map weighted images. The measured flow rate within ascending aorta is shown in Fig. 4 for various under-sampling rate. The results shows an excellent agreement on estimated flow for acceleration rates up to 4.

C. Real Time Flow in Ascending Aorta and Aortic Valve

In vivo real-time average through-plane blood flow velocity over multiple cardiac cycles in the ascending aorta is shown in Fig. 5. The average blood flow velocity was calculated over an ROI within the vessel and the motion of the vessel during the cardiac cycle was compensated by moving the ROI. The blood velocity measured with the real-time was compared with the gated sequence and showed excellent agreement with a slight underestimation of the peak blood flow due to averaging of blood flow through the cardiac phase.

In vivo real-time velocity image through aortic valve is shown in Fig. 6 with the magnitude image. The magnitude image is acquired in the separate acquisition with the spectral-spatial pulses to reduce the off-resonance effect and fat suppression. The blood flow velocity of a sample voxel through the valve is shown on the velocity map image.

V. CONCLUSION

We have shown a technique for high spatial and temporal resolution imaging of blood flow without cardiac gating. Temporal resolution of the flow images was improved by a factor of at least three with no cardiac gating signal with preserved spatial resolution. The adaptive B_1 map calculation from the raw data eliminates the need for an extra body coil scan. The SENSE reconstruction will result in lower SNR values and increase in reconstruction time. The technique can also be used for measuring the in-plane blood flow and imaging of the blood motion on patients with atrial fibrillation.

REFERENCES

[1] K.S. Nayak, J.M. Pauly, A.B. Kerr, B.S. Hu, and D.G. Nishimura, "Real-time color flow MRI," *Magn. Reson. Med.*, vol. 43, no. 2, pp. 251–258, 2000.

[2] P.D. Gatehouse, D.N. Firmin, S. Collins, and D.B. Longmore, "Real time blood flow imaging by spiral scan phase velocity mapping," *Magn. Reson. Med.*, vol. 31, no. 5, pp. 504–512, 1994.

[3] R.B. Thompson and E.R. McVeigh, "Real-time volumetric flow measurements with complex-difference MRI," *Magn. Reson.Med.*, vol. 50, no. 6, pp. 1248–1255, 2003.

[4] K.P. Pruessmann, M. Weiger, M.B. Scheidegger, and P. Boesiger, "SENSE: sensitivity encoding for fast MRI," *Magn. Reson. Med.*, vol. 42, no. 5, pp. 952–962, 1999.

[5] D.K. Sodickson and W.J. Manning, "Simultaneous acquisition of spatial harmonics (SMASH): fast imaging with radiofrequency coil arrays," *Magn. Reson. Med.*, vol. 38, no. 4, pp. 591–603, 1997.

[6] K.P. Pruessmann, M. Weiger, and P. Boesiger, "Sensitivity encoded cardiac MRI," *J. Cardiovasc. Magn Reson.*, vol. 3, no. 1, pp. 1–9, 2001.

[7] P. Thunberg, M. Karlsson, and L. Wigstrom, "Accuracy and reproducibility in phase contrast imaging using SENSE," *Magn Reson. Med.*, vol. 50, no. 5, pp. 1061–1068, 2003.

[8] F.T.A.W Wajer and K.P Pruessmann, "Major speedup of reconstruction for sensitivity encoding with arbitrary trajectories," *Proc. Intl. Soc. Mag. Reson. Med*, vol. 9, pp. 767, 2001.

[9] G.H. Golub and C.F. Van Loan , *"Matrix Computations"*, The Johns Hopkins Univ Press; 1996.

[10] J.I. Jackson, Mayer C.H, D. Nishimura, and A. Macovski, "Selection of convolution function for fourier inversion using gridding," *IEEE Trans. Med. Imaging*, vol. 10, no. 3, pp. 473–478, 1001.

[11] P. Kellman, F.H. Epstein, and E.R. McVeigh, "Adaptive sensitivity encoding incorporating temporal filtering (TSENSE)," *Magn. Reson. Med.*, vol. 45, no. 5, pp. 846–852, 2001.

[12] B. Madore, G.H. Glover, and N.J. Pelc, "Unaliasing by fourier-encoding the overlaps using the temporal dimension (UNFOLD), applied to cardiac imaging and fMRI," *Magn. Reson. Med.*, vol. 42, no. 5, pp. 813–828, 1999.

[13] D.O. Walsh, A.F. Gmitro, and M.W. Marcellin, "Adaptive reconstruction of phased array MR imagery," *Magn. Reson. Med.*, vol. 43, no. 5, pp. 682–690, 2000.

[14] M.A. Bernstein, A. Shimakawa, and N.J. Pelc, "Minimizing TE in moment-nulled or flow-encoded two- and three-dimensional gradient-echo imaging," *J.Magn. Reson. Imaging*, vol. 2, no. 5, pp. 583–588, 1992.

[15] C.H. Meyer, B.S. Hu, D.G. Nishimura, and A. Macovski, "Fast spiral coronary artery imaging," *Magn. Reson. Med.*, vol. 28, no. 2, pp. 202–213, 1992.

[16] C.H. Meyer, J.M. Pauly, A. Macovski, and D.G. Nishimura, "Simultaneous spatial and spectral selective excitation," *Magn. Reson. Med.*, vol. 15, no. 2, pp. 287–304, 1990.